Computer Assisted Mechanics and Engineering Sciences, 8: 155–168, 2001.

On the stability "in the large" and unsafe disturbances in a nonlinear oscillator

Wanda Szemplińska-Stupnicka, Elżbieta Tyrkiel
and Andrzej Zubrzycki
Institute of Fundamental Technological Research, Polish Academy of Sciences
ul. Świętokrzyska 21, 00-049 Warsaw, Poland

(Received December 7, 1999)

The problem of the stability "in the large" and the unsafe disturbances of the equilibrium position is studied for the structures whose dynamics is governed by the equation of motion of the pendulum with parametric excitation. The system displays a variety of nonlinear and chaotic phenomena, so that the study requires the use of theoretical concepts of the mathematics of chaos. Detailed explorations are performed by the aid of the nonlinear software package *Dynamics*.

1. Introduction

The problem of the stability of the steady-state oscillatory solutions became relevant to engineering design since it was realized that the nonlinear effects in dynamical devices may result in undesired responses, or even in the failure of the structure. The effects come from the fact that the nonlinear systems very often possess more than one solution at given values of the system control parameters, and that two or more solutions may be locally stable. The concept of the local stability is based on the assumption of *small disturbances* of the steady-state solution. This allows to drop the nonlinear terms in the variational equation of motion and, by the use of approximate methods, to derive simple criteria for the stability [8, 13, 20]. The criteria, however, are satisfactory merely to identify the unstable solutions, but are not efficient to assure stability of the solution. The problem is that the assumption of small disturbances is not satisfied in engineering devices, the devices which work in a noisy environment.

Consider the standard example of the single-degree-of-freedom damped oscillator, driven by the external harmonic force $P\cos\omega t$, with the nonlinear characteristics of the restoring force, assumed in the form

$$f_r = kx + \mu x^3$$

where x denotes displacement from the stable equilibrium position, k stands for the linear stiffness, and μx^3 represents nonlinear component of the spring force. For $\mu > 0$ the theoretical amplitude–frequency curves are bent towards higher frequency and hence, within the zone $\omega_2 < \omega < \omega_1$, three solutions coexist (Fig. 1a). The analysis of local stability indicates that the middle branch A–B is unstable, and that the two remaining solutions, S_r and S_n, are stable. Indeed, the system may execute oscillations with the higher resonant amplitude or with the lower nonresonant amplitude, depending on the initial conditions. If one starts with the initial conditions very close to the resonant oscillation and increases the frequency ω in a quasi-static manner, the condition of small disturbances from the steady state is satisfied, and the system continues to execute the S_r solution until the value $\omega = \omega_2$ is reached. Then the response "jumps" suddenly onto the low-amplitude nonresonant oscillation S_n. Analogously, on the decrease of the frequency, with the initial values $\omega > \omega_2$, the jump from the nonresonant to resonant solution occurs at $\omega = \omega_1$.

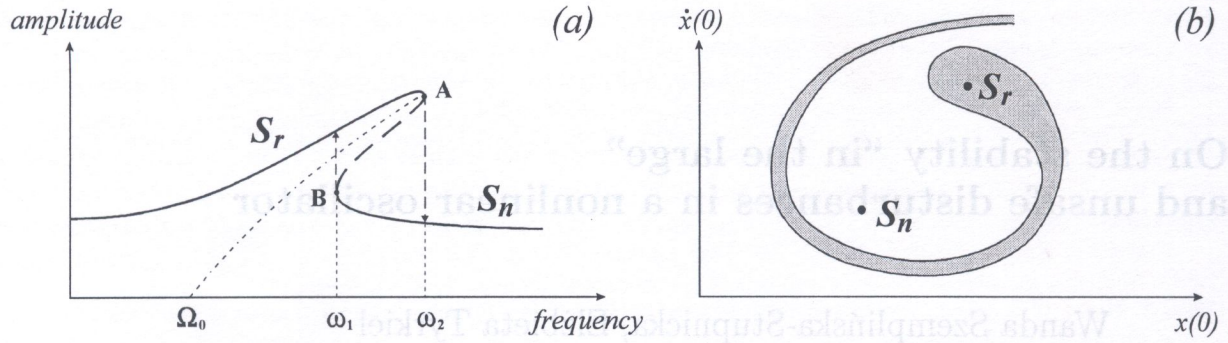

Fig. 1. Schematic diagram of: (a) amplitude–frequency curves and (b) basins of attraction at $\omega = \omega_2 - \Delta\omega$, $\Delta\omega \ll \omega_2$

The problem of the stability "in the large", i.e. the system behavior in the situation when the condition of small disturbances from the steady state was not satisfied, was studied by A. Tondl. The first results obtained by the aid of an analog computer have been published as early as 1966 [29, 30]. The problem was inspired by an undesired behavior of an engineering device. The mechanical model of the device was assumed in the form of the single-degree-of-freedom oscillator with the amplitude–frequency relation displayed in Fig. 1a. The device was supposed to work at the highest possible amplitude, i.e. in resonant condition with the frequency ω close to ω_2. It happened very often, however, that the amplitude suddenly dropped to the nonresonant branch at ω essentially lower than ω_2. A close look at the working conditions of the device revealed that the system was working in a noisy environment, and the system behavior was explained in terms of the new concept of the *basin of attraction*. We recall that, in dissipative systems, the basin of attraction of a steady-state stable solution (*attractor*) is a set of all initial conditions $(x(0), \dot{x}(0))$ that, after some transient motion, lead to the given attractor. It was shown that the basin of attraction of the resonant response S_r diminishes gradually when the frequency grows and approaches $\omega = \omega_2$. The schematic diagram of the basins of attraction of the resonant and nonresonant attractors S_r, S_n, at the frequency slightly lower than ω_2, is displayed in Fig. 1b. The diagram reveals that, although both attractors are still locally stable, the area of initial conditions that gives rise to transient trajectories which settle onto the resonant attractor S_r is much smaller than that which belongs to the nonresonant attractor S_n. It follows that even moderate disturbance of the S_r attractor may result in the trajectory that settles onto the nonresonant response S_n.

Recently the studies of the effects of large disturbances on the stability of the steady-state oscillations were extended to *chaotic systems* [7, 15, 26, 31]. In a series of papers, the potential energy of the considered mathematical model possessed one minimum and one maximum. The system was supposed to exhibit the oscillating motion within the potential well, but it could also exceed the potential barrier and escape to the "attractor at infinity". The former solution was regarded as the safe response, while the latter represented the unsafe one, the response that resulted in the failure of the structure. The problem was related to the studies of the ship capsize and earthquake damage [18, 19, 23, 24, 25, 27]. The system revealed occurrence of highly irregular chaotic phenomena and therefore required the use of the modern mathematical concepts of nonlinear dynamics, such as global bifurcations and bifurcations of the basin boundary. It was shown that the resulting fractal structure of the basins of attraction played a significant role in the problem of prediction of transient motion as well as of the final outcome, after large disturbance of the steady-state oscillations. We recall that the *fractal structure* is a highly intertwined, fine-scale structure with a fractional (non-integer) dimension greater than one, which involves basins of attraction of multiple coexisting attractors.

In this paper we study the problem of the unsafe response in the device governed by the equation of motion of the pendulum with parametric excitation. The importance of the pendulum in modelling engineering devices, such as offshore structures, buildings in earthquake or Josephson junction, makes its study of relevance to a wide audience of theoretical and applied scientists and engineers [1–5, 9, 11, 16, 17].

The system displays a variety of nonlinear and chaotic phenomena so that our study is based on the theoretical concepts of the mathematics of chaos, and detailed numerical exploration is performed by the use of the nonlinear software package *Dynamics* [14].

In the pendulum with parametric excitation the unsafe response corresponds to the *rotating solution*. We show that the nonlinear phenomena may result in the unsafe response even in the region of control parameters where the trivial solution, i.e. the hanging position, remains to be stable, and the linear analysis does not allow to predict existence of any other solution.

2. Equation of motion and zones of parametric instability

Mechanical model of the system considered is displayed in Fig. 2. It consists of a simple damped pendulum with mass m and length l, when base is subjected to a vertical sinusoidal time-history displacement $z(\tau)$. Equation of motion of the system, in terms of the angle x that defines the configuration, is

$$l^2 \frac{\mathrm{d}^2 x}{\mathrm{d}\tau^2} + \frac{c}{m}\frac{\mathrm{d}x}{\mathrm{d}\tau} + l\left(\frac{\mathrm{d}^2 z}{\mathrm{d}\tau^2} + g\right)\sin x = 0. \tag{1}$$

With the notations:

$$\Omega_0^2 \equiv \frac{g}{l}, \qquad t \equiv \Omega_0 \tau, \qquad h \equiv \frac{c}{\Omega_0 m l^2},$$

and the assumption

$$z(\tau) = -z\cos\bar{\omega}\tau,$$

Equation (1) is reduced to the form

$$\ddot{x} + h\dot{x} + (1 + p\cos\omega t)\sin x = 0 \tag{2}$$

where dots denote differentiating with respect to the nondimensional time t, and

$$\omega \equiv \frac{\bar{\omega}}{\Omega_0}, \qquad p \equiv \frac{z\omega^2}{l}.$$

In the mathematical equation of motion (Eq. (2)) x denotes the rotation angle in anti-clockwise direction from the lowest (hanging) position, h is the relative damping coefficient, and p, ω stand for the amplitude and frequency of the parametric excitation, respectively.

A significant peculiarity of the system with parametric excitation relies in existence of the stable trivial solution $x = \dot{x} = 0$ in a wide range of the system control parameters p, ω. The instability of

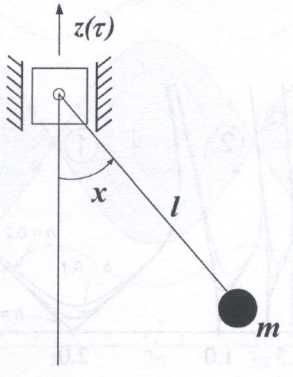

Fig. 2. Mechanical model of the pendulum with parametric excitation

the trivial solution is examined on assumption of small disturbances from the equilibrium, so that the disturbed solution $\tilde{x}(t)$ takes the form

$$\tilde{x}(t) = 0 + \delta x(t), \qquad \frac{\mathrm{d}\tilde{x}(t)}{\mathrm{d}t} = 0 + \delta\dot{x}(t).$$

Since the disturbances are small, the nonlinear terms for δx, δx^2 are neglected and the linear variational equation is considered,

$$\delta\ddot{x} + h\delta\dot{x} + \delta x(\omega_0^2 + p\cos\omega t) = 0, \tag{3}$$

with $\omega_0 = 1$, $T = \frac{2\pi}{\omega}$.

Because a closed form solution of the linear equation with parametric excitation is unobtainable, the Floquet theory is used to formulate general properties of the stability [8, 13, 20]. But quantitative results in the zones of parametric instability on the control parameter plane p–ω (at $h = \text{const}$) need application of computer based procedures. The final results are displayed in Fig. 3. The unstable regions on the p–ω plane, where the disturbances $\delta x(t)$ and hence the displacement $x(t)$ grow exponentially over time, are denoted (1), (2), (3)... For zero damping the unstable zones emanate from the ω axis at the values

$$\omega = \frac{2\omega_0}{k}, \qquad k = 1, 2, 3, \ldots \tag{4}$$

According to the Floquet theory, the solution takes the form

$$\delta x(t) \equiv x(t) = e^{(-\frac{h}{2} \mp \varepsilon)t}\,\Phi(t), \tag{5}$$

where $\Phi(t)$ is a periodic function of time with the period T or $2T$ ($T = \frac{2\pi}{\omega}$), and ε is an unknown characteristic exponent (purely real or purely imaginary) which is determined by numerical study.

The type of stability of the solution depends on the sign of the real part of the complete exponent $(-\frac{h}{2} \mp \varepsilon)$. When $\mathrm{Re}(-\frac{h}{2} \mp \varepsilon)$ is positive, the solution for $\delta x(t)$ grows exponentially over time, and therefore the trivial solution $x = \dot{x} = 0$ is unstable.

The diagram in Fig. 3 shows that the most dangerous region of the parameter p–ω plane is that around $\omega = 2$. This *principal unstable zone* is robust with respect to the damping coefficient and occupies a wide range in the control plane. In this zone the periodic function of time $\Phi(t)$ in Eq. (5) is $2T$-periodic.

In reality, the response $x(t)$ does not grow to infinity in the unstable regions, but, due to the nonlinear terms, remains bounded. For sufficiently low values of the parameter p the steady-state oscillating solution within the unstable region has the same form as that at the stability boundaries of the linearized system. It follows that within the principal unstable region around $\omega = 2$ the system exhibits oscillations of the period $2T \equiv 2\frac{2\pi}{\omega}$.

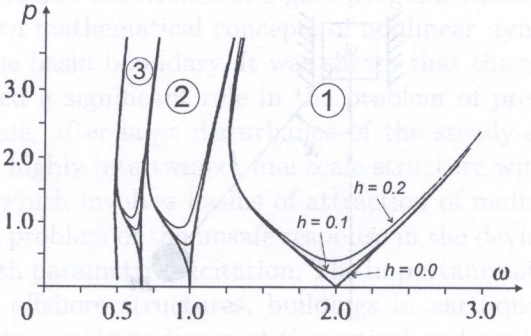

Fig. 3. Diagram of the parametric instability zones

The nonlinear term in the equation of motion (Eq. (2)) has a particular form, the form that the potential energy of the system is a periodic function of the displacement. If we assume zero value for the minimum of the energy, we obtain

$$V(x) = 1 - \cos x. \tag{6}$$

The potential energy (6) induces an additional type of the solution, namely the rotating solution. Thus the pendulum governed by Eq. (2), in the vicinity of $\omega = 2$, can

- remain in hanging position ($x = \dot{x} = 0$);
- oscillate around the hanging position with the period $2T$;
- rotate in clockwise or anti-clockwise direction.

The first two types of motion remain bounded and hence are regarded as *safe responses*, while the rotating solution represents the *unsafe response*, because it inevitably leads to a failure of the structure.

At this point it is useful to recall fundamental properties of free vibrations of the conservative, autonomous pendulum governed by the equation

$$\ddot{x} + \sin x = 0, \tag{7}$$

and to interpret trajectories on the phase-plane x–$\dot{x}$, in connection with the potential energy $V(x)$ [10, 20]. The hamiltonian pendulum (7) can also exhibit the above three types of motion (Fig. 4). Hanging position is represented by the single points (*centers*) at $x = 2\pi n$, $n = 0, 1, 2, \ldots$, oscillating motion — by the ellipse-shaped, close trajectories, and the rotating motion — by the wave-form trajectories which satisfy the condition of unchanged sign of the velocity. The other singular points, at $x = (2n-1)\pi$, $n = 0, 1, 2, \ldots$, correspond to the unstable, inverted position of the pendulum and are defined as *hilltop saddles*. The particular trajectories that seem to leave or approach the hilltop saddles can not be realized in the system in finite time and are defined as

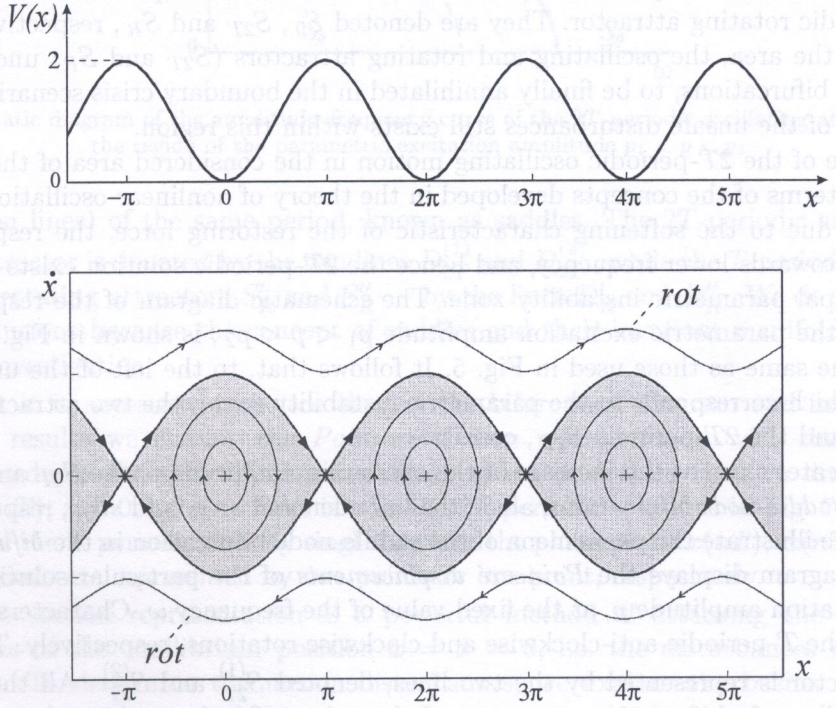

Fig. 4. Potential energy and the phase portrait of the undamped, autonomous pendulum

invariant manifolds of the saddles. They play the role of *separatrix*, i.e. the lines that separate the oscillating and rotating motion in the phase plane.

In the considered undamped, autonomous system the criterion for the rotating motion to occur is very simple; the system will exhibit rotating motion when its initial mechanical energy exceeds the maximum value of the potential energy,

$$E(0) > V_{\max} = 2.$$

Turning back to the damped pendulum under parametric excitation (Eq. (2)) we notice that our problem of the criterion for the unsafe disturbances is analogous to that of the separatrix, i.e. the boundary between the bounded and unbounded responses. The nonautonomous system governed by Eq. (2) is, however, three dimensional and can exhibit irregular, chaotic phenomena. The problem becomes very complex and requires extensive exploration.

3. Coexistence of the equilibrium, oscillating and rotating attractors; criteria for unsafe disturbances

In this section we first consider the steady-state responses of the parametrically driven pendulum (Eq. (2)) in the region of the control parameters p–ω where the equilibrium hanging position remains to be stable and, therefore, linear analysis does not give any warning about unsafe disturbances. In the neighborhood of the principal parametric instability there is, however, a region where, in addition to the locally stable equilibrium attractor, the oscillating $2T$-periodic and the rotating T-periodic attractors coexist. Which one of the three steady-state responses is realized in the system it depends on the initial conditions. If our starting point is the equilibrium position $x = \dot{x} = 0$, then "the initial conditions" correspond to the disturbances applied to the system, and the unsafe disturbances are those which lead to the rotating motion.

Results of computer exploration of the steady-state responses (attractors) of the system, in the neighborhood of the principal parametric instability zone close to $\omega = 2$, are displayed in Fig. 5. The region of interest is the triangle-like area denoted A–B–C. In the portion of the area marked in dark grey, there coexist: the equilibrium ($x = \dot{x} = 0$) attractor, the $2T$-periodic oscillating attractor, and the T-periodic rotating attractor. They are denoted S_0, S_{2T} and S_R, respectively. In the light grey portion of the area, the oscillating and rotating attractors (S_{2T} and S_R) undergo a series of period-doubling bifurcations, to be finally annihilated in the boundary crisis scenario [6, 21, 22, 28]. Yet, the danger of the unsafe disturbances still exists within this region.

The existence of the $2T$-periodic oscillating motion in the considered area of the p–ω plane can be explained in terms of the concepts developed in the theory of nonlinear oscillations [4, 8, 10, 20]. It follows that, due to the softening characteristic of the restoring force, the response–frequency curves are bent towards lower frequency, and hence the $2T$-periodic solution exists also outside the V-shaped principal parametric instability zone. The schematic diagram of the response–frequency curve, valid for the parametric excitation amplitude $p_1 < p < p_2$, is shown in Fig. 6. Notations in the figure are the same as those used in Fig. 5. It follows that, to the left of the unstable segment of the ω-axis (which corresponds to the parametric instability zone), the two attractors, namely the equilibrium S_0 and the $2T$-periodic S_{2T}, coexist.

Figure 5 indicates that, at the increase of the excitation amplitude p, the S_{2T} and S_R attractors are born in the *saddle-node bifurcations*, along the lines denoted sn_{2T} and sn_R, respectively. For the sake of clarity, we illustrate the phenomena of the saddle-node bifurcation in the *bifurcation diagram* (Fig. 7). The diagram displays the *Poincaré displacements* of the particular solutions against the parametric excitation amplitude p, at the fixed value of the frequency ω. Characters S'_R and S''_R are used to denote the T-periodic anti-clockwise and clockwise rotations, respectively. The $2T$-periodic oscillating attractor is represented by the two lines, denoted $S^{(1)}_{2T}$ and $S^{(2)}_{2T}$. All the attractors are born in the saddle-node bifurcation scenarios, at the values of p denoted $p_{sn_{2T}}$ and p_{sn_R}. At this type of local bifurcation, the stable branches (solid lines) are always accompanied by the unstable

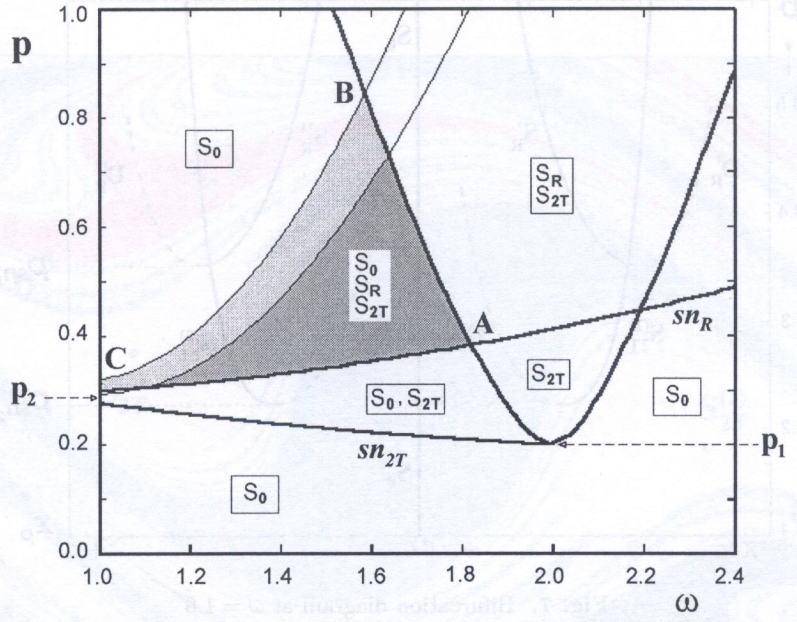

Fig. 5. Regions of coexistence of the locally stable steady-state responses (attractors) in the control plane; S_0 — equilibrium ($x = \dot{x} = 0$) attractor, S_{2T} — $2T$-periodic oscillating attractor, S_R — T-periodic rotating attractor

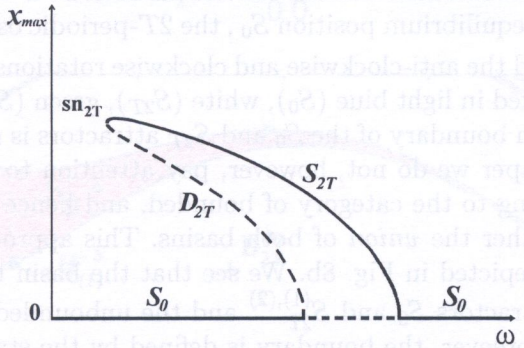

Fig. 6. Schematic diagram of the amplitude–frequency curve of the $2T$-periodic oscillating attractor S_{2T}, in the region of the parametric excitation amplitude $p_1 < p < p_2$

branches (broken lines) of the same period, known as saddles. The $2T$-periodic saddle associated with the S_{2T} attractor is denoted by the two lines $D^{(1)}_{2T}$ and $D^{(2)}_{2T}$, while the T-periodic saddles which accompany the rotating attractors S'_R and S''_R — by the lines D'_R and D''_R. We do pay attention to the unstable solutions because the concept of saddles and their invariant manifolds play a crucial role in further investigation.

At this point it is necessary to notice that in the bifurcation diagram and in presentation of the subsequent results we employ the *Poincaré section representation* with the sampling time $T = \frac{2\pi}{\omega}$. This reduces the three dimensional state space $(x, \dot{x}, t)$ to the two dimensional phase plane $x(nT), \dot{x}(nT)$, $n = 0, 1, 2, \ldots$. That is why the $2T$-periodic solutions in Fig. 7 are represented by two lines, and the T-periodic ones by single lines. In the phase plane $x(nT)$, $\dot{x}(nT)$ the two types of periodic solutions are represented by two points or one point, respectively.

The Poincaré section representation is a powerful method of attacking the problem of unsafe disturbances of the equilibrium position $x = \dot{x} = 0$, i.e. the disturbances that lead to rotating solutions. To determine the unsafe disturbances, we explore the basins of attraction of the safe and unsafe attractors of the system. In our case, the basin of attraction of an attractor S_i $(i = 0, 2T, R)$ is equivalent to the set of all initial disturbances of the equilibrium

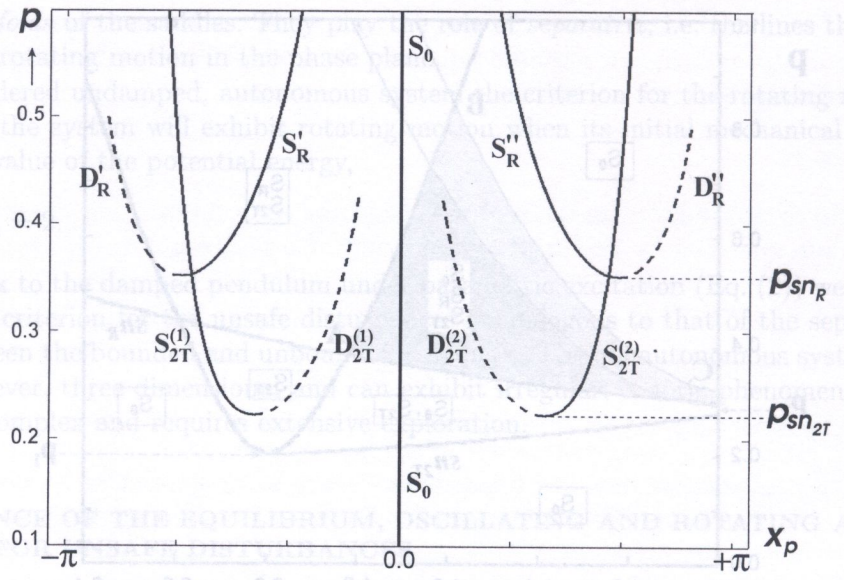

Fig. 7. Bifurcation diagram at $\omega = 1.6$

solution $x = \dot{x} = 0$ that give rise to the trajectories which settle finally onto the attractor S_i.

We begin with the basins of attraction at the control parameters $\omega = 1.6$, $p = 0.44$ (Fig. 8a). The coexisting attractors are the equilibrium position S_0, the $2T$-periodic oscillation S_{2T} (represented by two points $S_{2T}^{(1)}$ and $S_{2T}^{(2)}$), and the anti-clockwise and clockwise rotations S'_R, S''_R. The corresponding basins of attraction are marked in light blue (S_0), white (S_{2T}), green (S'_R) and magenta (S''_R) colors. First we notice that the basin boundary of the S_0 and S_{2T} attractors is not smooth, but has a fractal structure [12, 21]. In this paper we do not, however, pay attention to the observation because the two involved attractors belong to the category of bounded, and hence safe, responses. Therefore it is reasonable to consider rather the *union* of both basins. This approach reduces the complicated form of the basins to that depicted in Fig. 8b. We see that the basin boundary between the union of the two bounded, safe attractors S_0 and $S_{2T}^{(1),(2)}$ and the unbounded rotating attractors S'_R, S''_R is a smooth, regular line. Moreover, the boundary is defined by the stable manifolds of the saddles D'_R, D''_R, denoted $W^s_{(1)}$ (blue line) and $W^s_{(2)}$ (red line), respectively. Thus we notice that, in the case of coexistence of the non-rotating and rotating attractors, there are the stable manifolds of the saddles accompanying the rotating attractors which play the role of the *separatrix*.

The basins of attraction displayed in Fig. 8b enable us to make the following observation on the unsafe disturbances, i.e. unsafe initial conditions. If we assume $\dot{x}(0) = 0$, then all initial displacements $x(0) \leq |\pi|$ give rise to trajectories that settle on the safe attractors, and therefore belong to the category of safe disturbances. It follows that in this case no initial displacement can lead to the unbounded rotating motion of the pendulum.

However, a small increase of the parametric excitation amplitude p brings a sudden dramatic change of the situation. Results of numerical computations of basins of attraction at the values of control parameters $\omega = 1.6$, $p = 0.52$ are displayed in Figs. 9a,b. Now the initial conditions that result in the rotating response invade the area that belonged entirely to the safe attractors. The basin boundary is no longer smooth but it has fractal structure. The regular, smooth portion of the safe basin is now reduced to the basin of the equilibrium attractor S_0. If we follow the assumption of the zero initial velocity, the safe initial displacement is now reduced to $x(0) \preceq |0.5|$.

To determine the criteria for the threshold values of the parameters p, ω for which the sudden decrease of the basin of safe disturbances occurs we first notice that the process begins with the bifurcation of the basin boundaries and consequently with generating fractal structure of the basins. Since we remember that, prior to the bifurcation, the basin boundary between the non-rotating

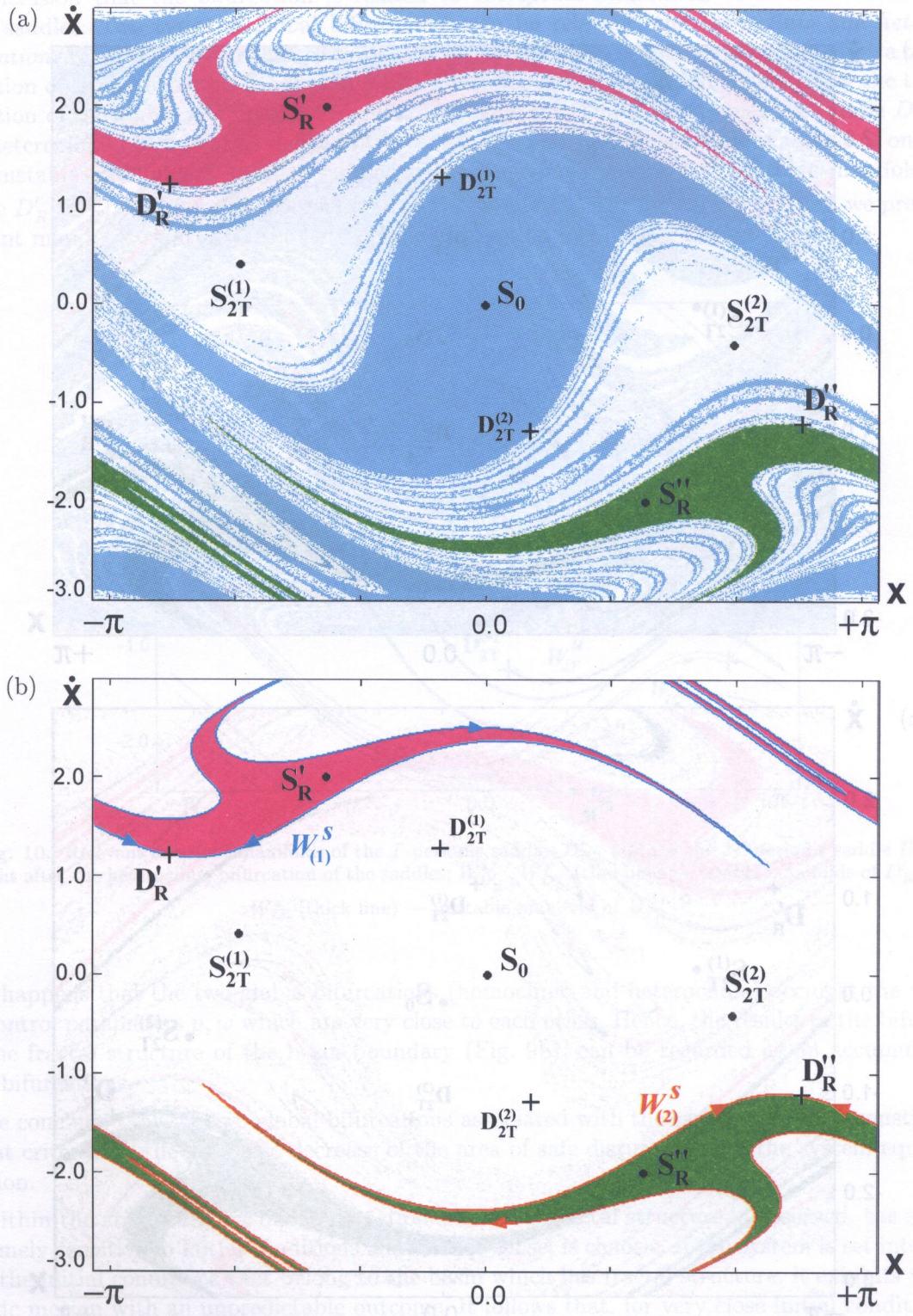

Fig. 8. Basins of attraction of the coexisting attractors at $\omega = 1.6$, $p = 0.44$; (a) light blue — basin of the equilibrium ($x = \dot{x} = 0$) attractor S_0, white — basin of the $2T$-periodic oscillating attractor S_{2T}, magenta and green — basins of the two T-periodic rotating attractors, anti-clockwise S'_R and clockwise S''_R, respectively; (b) basin of the union of S_0 and S_{2T} attractors (white) and basins of the rotating attractors S'_R and S''_R. The grid resolution is 640 × 480

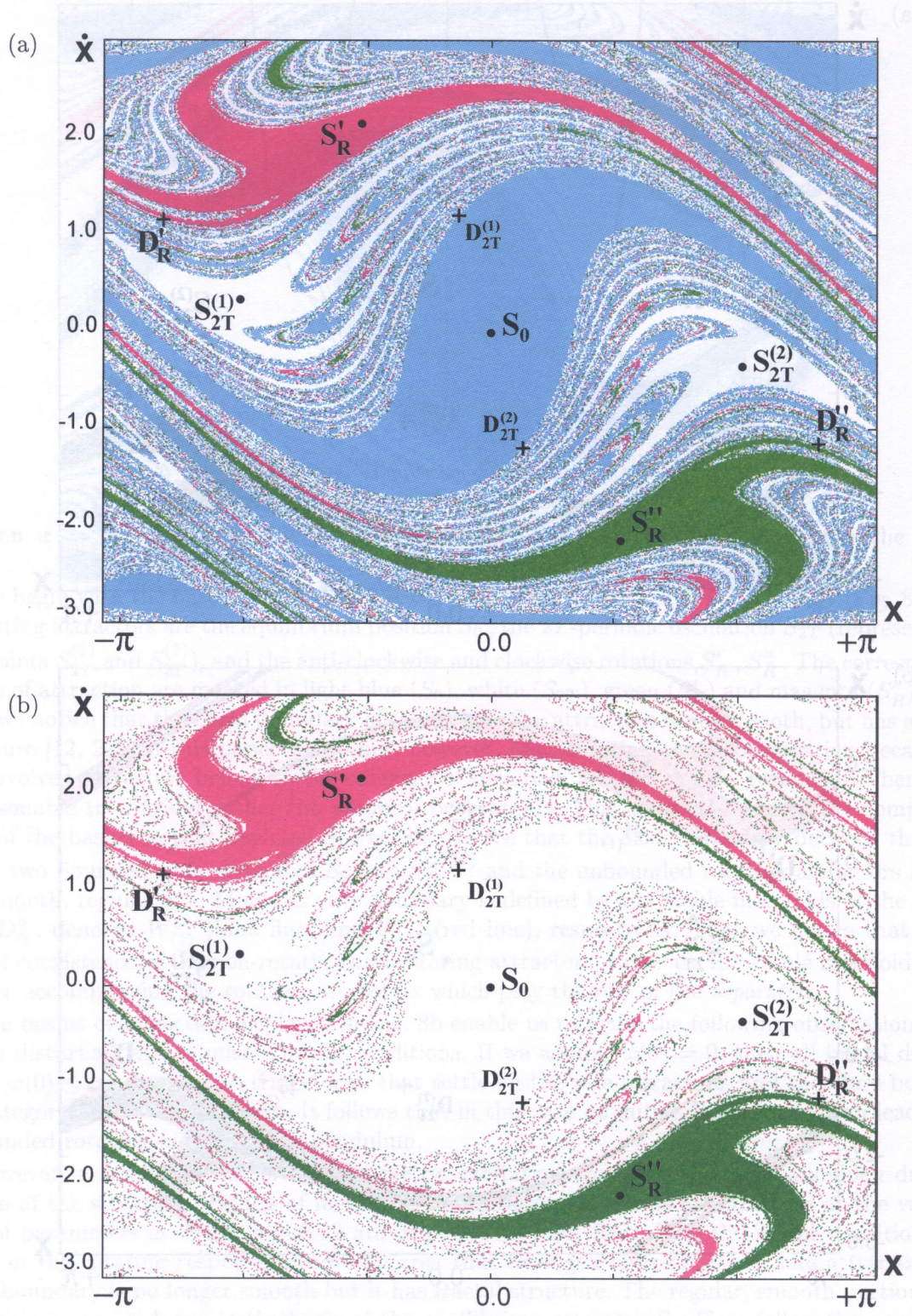

Fig. 9. Basins of attraction of the coexisting attractors at $\omega = 1.6$, $p = 0.52$; (a), (b) color correspondence and grid resolution as in Fig. 8a,b

and rotating attractors was defined by the stable manifolds of the saddles D'_R, D''_R, we come to conclusion that the bifurcation is related to the global bifurcation of invariant manifolds of these saddles. Two types of global bifurcations can be relevant: the *homoclinic and heteroclinic bifurcations* [7, 21, 23, 31]. Critical conditions of the global bifurcations are determined by a tangency condition of the involved invariant manifolds. The homoclinic bifurcation is defined by the tangency condition of the stable and unstable manifolds of the same saddle, in our case the saddle D'_R (D''_R). The heteroclinic bifurcation is defined by a tangency condition of the stable manifold of one saddle and unstable manifold of another saddle; in the considered case it is the stable manifold of the saddle D'_R (D''_R) and the unstable manifold of the saddle $D_{2T}^{(1),(2)}$. For an illustration, we present the relevant manifolds right after the heteroclinic bifurcation in Fig. 10.

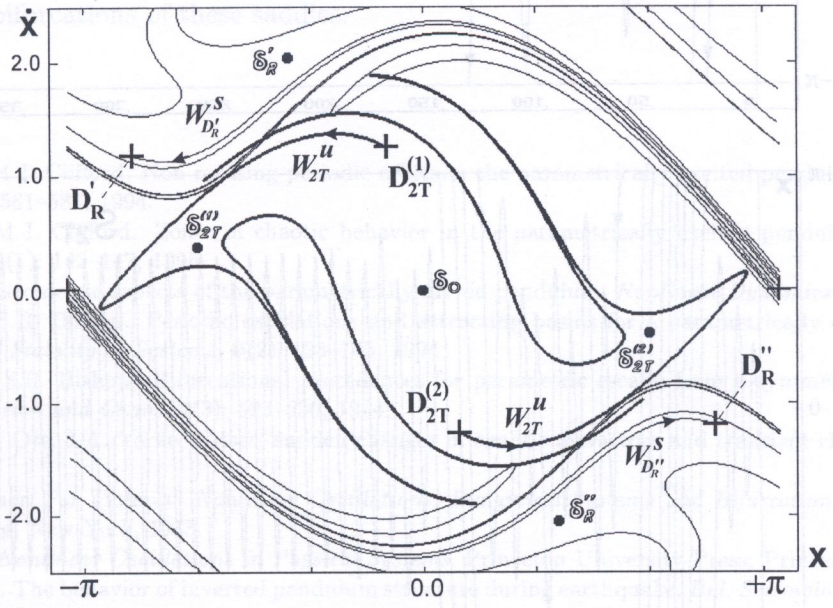

Fig. 10. Relevant invariant manifolds of the T-periodic saddles D'_R, D''_R and the $2T$-periodic saddle $D_{2T}^{(1),(2)}$, right after the heteroclinic bifurcation of the saddles; $W^s_{D'_R}$, $W^s_{D''_R}$ (thin lines) — stable manifolds of D'_R, D''_R; W^u_{2T} (thick line) — unstable manifold of $D_{2T}^{(1),(2)}$

It happens that the two global bifurcations (homoclinic and heteroclinic) occur at the values of the control parameters p, ω which are very close to each other. Hence, the results of the bifurcation, i.e. the fractal structure of the basin boundary (Fig. 9b), can be regarded as an accumulation of both bifurcations.

We conclude that the two global bifurcations associated with the saddles D'_R, D''_R constitute the sought criteria for the dramatic decrease of the area of safe disturbances of the system equilibrium position.

Within the area of the basins of attraction where the fractal structure is observed, the system is extremely sensitive to initial conditions and, in this sense, is chaotic. If the system is set into motion with the initial conditions that belong to the basin which has fractal structure, it exhibits transient chaotic motion with an unpredictable outcome. It follows that, for very close initial conditions, the system may either settle onto one of the safe, non-rotating attractors, S_0 or S_{2T}, or develop the unbounded rotating motion. The phenomena are illustrated by the time histories of the transient and final steady-state responses $x = x(t)$ realized with very close initial conditions — Fig. 11. After chaotic transients of arbitrary duration, the system settles onto the equilibrium attractor S_0 (Fig. 11a), the $2T$-periodic oscillating attractor S_{2T} (Fig. 11b), or onto the rotating attractor S'_R (Fig. 11c).

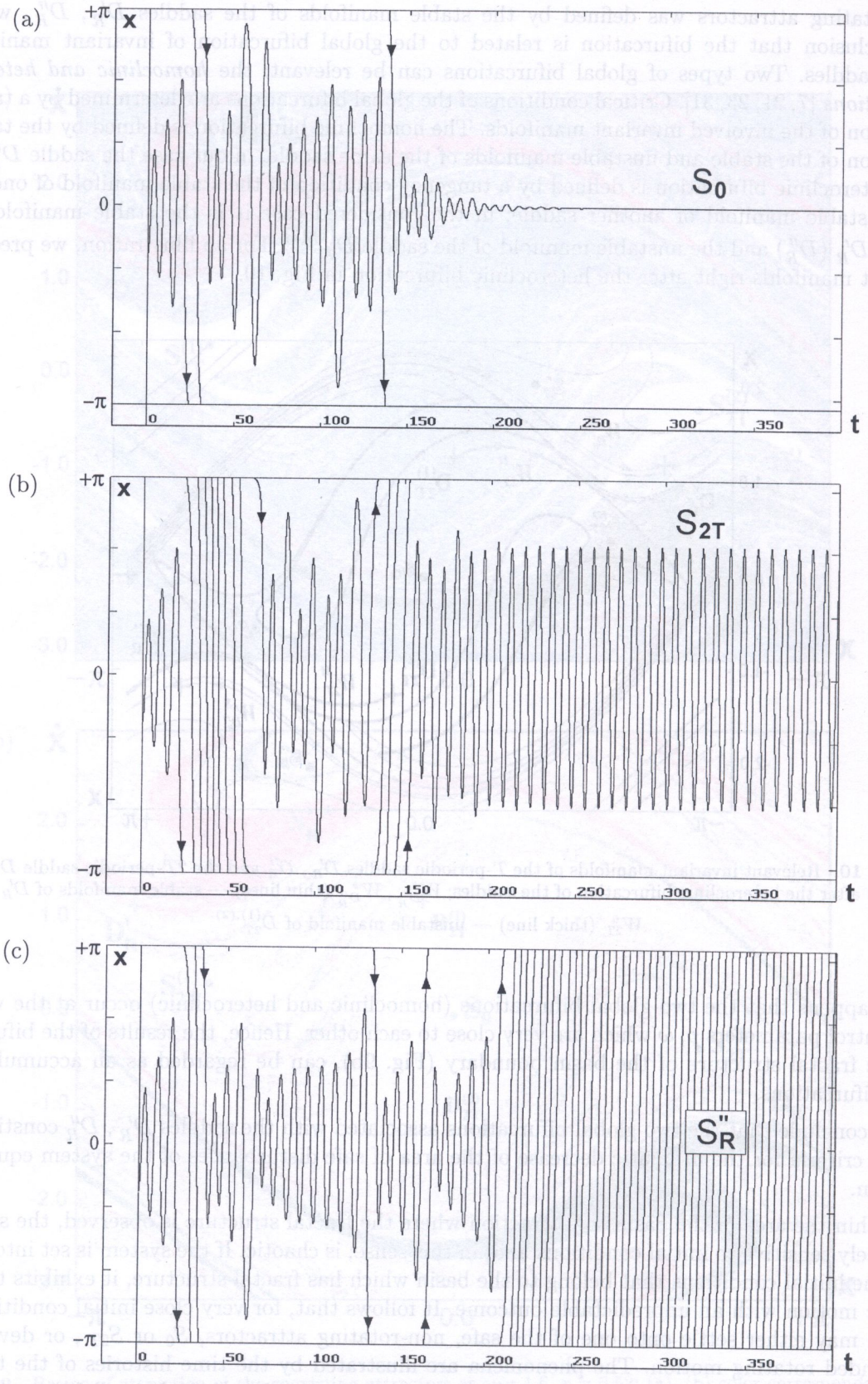

Fig. 11. Three time-histories of the system response with an unpredictable final outcome, at $\omega = 1.6$, $p = 0.52$, for the very close initial conditions which belong to the fractal region of the phase plane; (a) $x(0) = -0.767$, $\dot{x}(0) = 0.00$; (b) $x(0) = -0.767$, $\dot{x}(0) = 0.00$; (c) $x(0) = -0.761$, $\dot{x}(0) = 0.02$; (a), (b) — safe outcomes, (c) — unsafe outcome

4. Conclusions

Explorations of the regular and chaotic steady-state and transient responses of the nonlinear, parametrically excited pendulum, in connection with the study of global bifurcations, allow us to state that:

- investigations of the stability "in the large" and the unsafe disturbances require applications of the dynamics of chaos and computer aided methods;
- the sudden decrease of the values of the safe disturbances is related to the global bifurcations of the unstable rotating solutions, i.e. the saddles that accompany the rotating attractors; the critical values of the system control parameters p, ω are determined by the homoclinic and heteroclinic bifurcations of these saddles.

References

[1] S.R. Bishop, M.J. Clifford. Non rotating periodic orbits in the parametrically excited pendulum. *Eur. J. Mech. A/Solids*, **17**: 581–587, 1994.

[2] S.R. Bishop, M.J. Clifford. Zones of chaotic behavior in the parametrically excited pendulum. *J. Sound and Vibration*, **189**(1): 142–147, 1996.

[3] D. Capecchi. Geometric aspects of the parametrically driven pendulum. *Nonlinear Dynamics*, **7**: 231–247, 1995.

[4] D. Capecchi, S.R. Bishop. Periodic oscillations and attracting basins for a parametrically excited pendulum. *Dynamics and Stability of Systems*, **9**(2): 123–143, 1994.

[5] M.J. Clifford, S.R. Bishop. Bifurcational precedences for parametric escape from a symmetric potential well. *Int. J. Bifurcation and Chaos*, **4**(3): 623–630, 1994.

[6] C. Grebogi, E. Ott, J.A. Yorke. Crises, sudden changes in chaotic attractors and transient chaos. *Physica*, **D7**: 181–200, 1983.

[7] J. Guckenheimer, P.J. Holmes. *Nonlinear Oscillations, Dynamical Systems and Bifurcations of Vector Fields.* Springer-Verlag, New York, 1983.

[8] Ch. Hayashi. *Nonlinear Oscillations in Physical Systems.* Princeton University Press, Princeton, N.J., 1985.

[9] G.W. Housner. The behavior of inverted pendulum structure during earthquake. *Bul. Seismological Soc. America*, **53**: 403–417, 1963.

[10] S. Kaliski. *Vibrations and Waves.* PWN, Warsaw, Polish edition 1964, English edition 1985.

[11] B.P Koch, R.W. Leven. Subharmonic and homoclinic bifurcations in a parametrically forced pendulum. *Physica* **D16**: 1–13, 1985.

[12] S.W. McDonald, C. Grebogi, E. Ott, J.A. Yorke. Fractal basin boundaries. *Physica*, **D17**: 125–153, 1985.

[13] N. Minorski. *Nonlinear Oscillations.* Nostrand Comp., New York, 1962.

[14] H.E. Nusse, J.A. Yorke. *Dynamics: Numerical Explorations.* Springer-Verlag, New York, 1998.

[15] E. Ott. *Chaos in Dynamical Systems.* Cambridge University Press, Cambridge, 1993.

[16] R.C.T. Rainey. The dynamics of tethered platform. *Trans. Roy. Inst. Naval Architects*, **420**: 59–80, 1978.

[17] F.M. Salam, S.S. Sastry. Dynamics of the forced Josephson junction — the region of chaos. *IEEE Trans. Circuits and Systems CAS*, **30**: 784–796, 1985.

[18] M.S. Soliman. Predicting regimes of indeterminate jumps to resonance by assessing fractal boundaries in control space. *Int. J. Bifurcation and Chaos*, **4**(6): 1645–1653, 1994.

[19] M.S. Soliman, J.M.T. Thompson. Integrity measures quantifying the erosion of smooth and fractal basins of attraction. *J. Sound and Vibration*, **135**(3): 453–467, 1989.

[20] W. Szemplińska-Stupnicka. *The Behavior of Nonlinear Vibrating Systems*; vol. I — *Fundamental Concepts and Methods: Applications to Single-Degree-of-Freedom Systems.* Kluwer Academic Publishers, Dordrecht–Boston–London, 1990.

[21] W. Szemplińska-Stupnicka, E. Tyrkiel. Sequences of global bifurcations and the related outcomes after crisis of the resonant attractor in a nonlinear oscillator. *Int. J. Bifurcation and Chaos*, **7**(11): 2437–2457, 1997.

[22] W. Szemplińska-Stupnicka, A. Zubrzycki, E. Tyrkiel. Properties of chaotic and regular boundary crisis in dissipative driven nonlinear oscillators. *Nonlinear Dynamics*, **19**: 19–36, 1999.

[23] W. Szemplińska-Stupnicka, E. Tyrkiel. Effects of multi global bifurcations on basin organization, catastrophes and final outcomes in a driven nonlinear oscillator at the $2T$-subharmonic resonance. *Nonlinear Dynamics*, **17**: 41–59, 1998.

[24] J.M.T. Thompson. Chaotic phenomena triggering the escape from the potential well. *Proc. Roy. Soc. Lond.*, **A421**: 195–225, 1989.

[25] J.M.T. Thompson. Loss of engineering integrity due to erosion of absolute and transient basin boundaries. In: W. Schiehlen, ed., *Nonlinear Dynamics in Engineering Systems*, 313–320. Springer-Verlag, Berlin, 1990.
[26] J.M.T. Thompson, H.B. Stewart. *Nonlinear Dynamics and Chaos*. John Wiley and Sons, Chichester, 1986.
[27] J.M.T. Thompson, M.S. Soliman. Fractal control boundaries of driven oscillators and their relevance to safe engineering design. *Proc. Roy. Soc. Lond.*, **A428**: 1–13, 1990.
[28] J.M.T. Thompson, H.B. Stewart, Y. Ueda. Safe, explosive and dangerous bifurcations in dissipative dynamical systems. *Phys. Rev.*, **E 49**(2): 1019–1027, 1994.
[29] A. Tondl. A method of solving stability "in the large" with the aid of analog computers. *Acta Technica CSAV*, **5**: 576–597, 1966.
[30] A. Tondl. Domains of attraction for nonlinear systems. *Monographs and Memoranda*, Bechovice, **11**, 1970.
[31] S. Wiggins. *Introduction to Applied Nonlinear Dynamical Systems and Chaos*. Springer-Verlag, New York, 1990.